U.S. FOOD & DRUG ADMINISTRATION

Application of Metabolomic Analysis towards the Discovery of Biomarkers of Immunogenicity and Efficacy of Parasitic Vaccines

Azodi, Nazli, FDA/CBER/OBRR; Oljuskin, Timur, USDA; Markle, Hannah, FDA/CBER/OBRR; Bhattacharya, Parna, FDA/OHTVII/CDRH; Volpedo, Greta, Ohio State University; Satoskar, Abhay, Ohio State University; Gannavaram, Sreenivas, FDA/CBER/OBRR; Nakhasi, Hira, FDA/CBER/OBRR

ABSTRACT

Leishmaniasis is a parasitic disease that is prevalent in approximately 88 countries, and yet no licensed human vaccine exists against it. Towards control of leishmaniasis, we have developed *Leishmania major Centrin* gene deletion mutant strains (*LmCen*$^{-/-}$) as a live attenuated vaccine, which induces a strong Th1 response to provide IFN-γ-mediated protection to the host (Zhang et al, 2020). However, the immune mechanisms of such protection remain to be understood. Metabolomic reprogramming of the host cells following *Leishmania*-infection has been shown to play a critical role in pathogenicity and shaping the immune response following infection (Nagy & Haschemi, 2015). Here, we applied untargeted mass spectrometric analysis to study the metabolic changes induced by infection with *LmCen*$^{-/-}$ and compared them with virulent *L. major* parasite infection to identify the immune mechanism of protection.
Our data shows that immunization with *LmCen*$^{-/-}$ parasites, in contrast to virulent *L. major* infection, alters the tryptophan metabolism pathway to down-regulate the anti-inflammatory Kynurenine-AhR and FICZ-AhR signaling cascades, while promoting a pro-inflammatory response via increased melatonin synthesis.

INTRODUCTION

Leishmania parasites can be transmitted to humans via the bite of an infected sandfly or blood transfusions. Leishmaniasis causes significant morbidity and mortality worldwide with approximately one billion people globally at risk of infection. In recent years, autochthonous infections have been reported in the southern regions of the United States, marking the U.S. as an endemic country for leishmaniasis.

Figure 1. Leishmaniasis incurs a heavy global burden. Leishmaniasis infections are most commonly found in tropical regions, the middle east, and the Mediterranean countries. With the report of autochthonous infections in the southern regions of the United States, the U.S. has recently been classified as an endemic nation for leishmaniasis as well.

No FDA-approved vaccines or donor screening assays exist, and treatment options remain limited. The goal of this study was to analyze the metabolic changes associated with the *LmCen*$^{-/-}$ strain, a live attenuated vaccine candidate for leishmaniasis, in order to identify the immune mechanism of protection and metabolic biomarkers of immunogenicity.

METHOGOLOGY

C57/Bl6 mice were infected with wild type *L. major* (*LmWT)*and *LmCen*$^{-/-}$. The infected ear tissues were collected 7 days post infection and analyzed by untargeted LC/MS mass spectrometry, and the data were analyzed with the Metaboanalyst 5.0 (Xia et al. 2009, Pang et al. 2022) for pathway analysis and Metscape 3.1.1 (Karnovsky et al. 2012) for integrative network analysis. To verify the results from MS analysis, murine bone marrow-derived dendritic cells, were infected with *LmWT* and *LmCen*$^{-/-}$. To test the role of the kynurenine pathway in *Leishmania* immunity, BMDCs were cultured with 1-Methyl tryptophan, an IDO-1 inhibitor, or L-kynurenine and the expression levels of IDO-1, AhR, and IFN-γ were measured via qRT-PCR. To test the role of the indole pathway in *Leishmania* immunity, BMDCs were cultured with FICZ, the product of Indole-3-acetaldehyde that acts as an agonist of AhR, and the expression levels of AhR and IL-10 were measured via qRT-PCR. Lastly, to test the role of the serotonin pathway in *Leishmania* immunity, 4-CDP, an inhibitor of the rate-limiting enzyme in melatonin synthesis (TPH), was applied to the BMDCs, and the expression levels of IL-12 and TNF- α were measured by qRT-PCR.

RESULTS

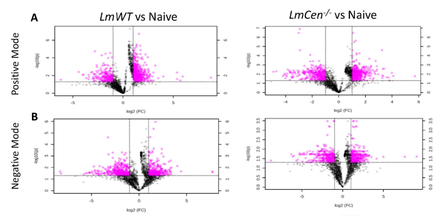

Figure 2. Infection with *LmWT* and immunization with *LmCen-/-* display distinct metabolic signatures at the inoculation site. Normalized data from ear tissue of C57Bl/6 mice was used to perform statistical analysis, and the *P*-values were obtained using an unpaired t test. Features selected by volcano plot with < 0.05 false-discovery rate (FDR) and > 2-fold change (FC) threshold cutoffs from positive **(A)** and negative modes **(B)** for ear tissue of *LmWT* vs. naïve AND *LmCen-/-* vs. naïve with log-transformed fold change (x) 2 and t-tests thresholds (y) 0.05

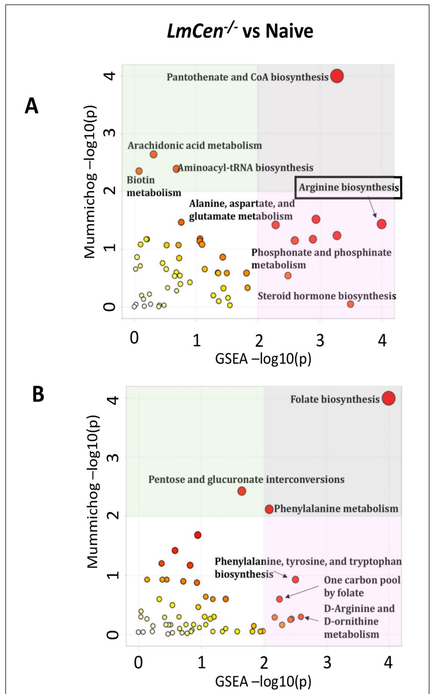

Figure 3. Metabolic pathways enriched in mice ear tissue infected with *LmWT* or immunized with *LmCen*$^{-/-}$. Normalized data from ear tissue of C57Bl/6 mice after 7 days of infection with *LmWT,* immunization with *LmCen*$^{-/-}$ or naïve control was used to perform peaks to pathway analysis. Using the MS Peaks to Paths module in MetaboAnalyst5.0, the mummichog and gene set enrichment analysis (GSEA) p-values were combined. The Integrated MS Peaks to Paths plot summarizes the results of the Fisher's method for combining mummichog (y) and GSEA (x) p-values from the positive **(A)** negative **(B)** mode data sets, indicating the metabolic pathways enriched. The size and color of the circles correspond to their transformed combined p-values. Large and red circles are considered the most perturbed pathways. The colored areas show the significant pathways based on either mummichog (green) or GSEA (pink), and the gray area highlights significant pathways identified by both algorithms. Arginine metabolism pathway associated with a protective immune response was found to be enriched in *LmCen*$^{-/-}$ immunization (highlighted by the black boxes).

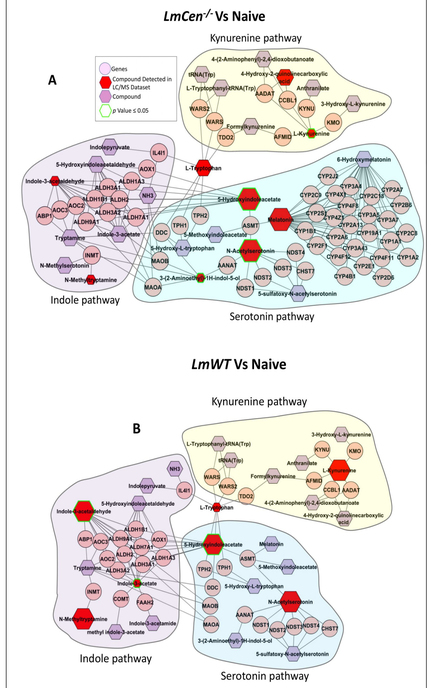

Figure 4. Infection with *LmWT and LmCen*$^{-/-}$ lead to differential regulation of the tryptophan metabolism pathway. Normalized data from the ear tissue of C57Bl/6 mice infected with *LmWT,* immunized with *LmCen*$^{-/-}$ and naïve controls was used to perform integrative compound-compound network analysis with Metscape. The differential regulation of the tryptophan metabolites, specifically kynurenine, indole-3-acetaldehyde, and melatonin are illustrated in this graph for the immunized **(A)** and infected **(B)** conditions compared to naïve control. Larger hexagons represent up-regulation, while smaller hexagons represent down-regulation. Red hexagons represent compounds detected in the data set, while hexagons with a green outline represent statistically significant metabolites (p-value ≤ 0.05). The purple hexagons represent compounds that are associated with the pathway but are not detected in the input dataset. The pink circles represent the genes regulating the biosynthetic activities. The networks associated with the kynurenine, indole, and serotonin pathways are highlighted with yellow, purple, and blue hues respectively.

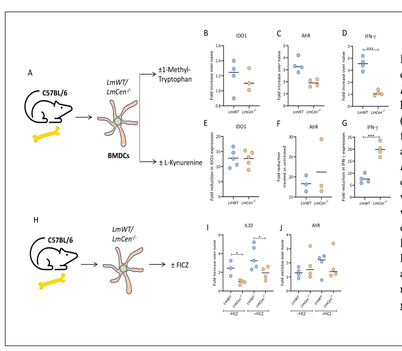

Figure 5. Validation of the role of kynurenine and FICZ in vaccine induced immunity. To confirm kynurenine-dependent alteration of IDO-1, AhR, and IFN-γ expression in *LmWT* and *LmCen*$^{-/-}$ infections, BMDCs were infected overnight with *LmWT* or *LmCen*$^{-/-}$ **(A)**. After 24 hours, 1-methyl tryptophan or kynurenine were added, and the expression levels of IDO-1 **(B)**, AhR **(C)**, and IFN-γ **(D)** were measured by RT-PCR. Treated naïve BMDCs were used forcalculating fold enrichment of the analytes. Upon the addition of 1-MT, in both *LmCen*$^{-/-}$ and the *LmWT* infections, the expression of AhR **(C)** and IFN-γ **(D)** were increased. Both *LmCen*$^{-/-}$ and *LmWT* infections showed a decrease in IDO1 **(E)**, AhR **(F)** and IFN-γ **(G)** expression upon the addition of kynurenine, showing that the expression of AhR and IFN-γ were kynurenine-dependent. To confirm the role of FICZ in the induction of IL-10, BMDCs were infected overnight with *LmWT* or *LmCen*$^{-/-}$ **(H)**. After 24 hours, FICZ was added, and the expression levels of IL-10 **(I)** and AhR **(J)** were measured by RT-PCR. Upon the addition of FICZ, in both *LmCen*$^{-/-}$ and the *LmWT* infections, the expression of IL-10 was increased **(I)**. Both *LmCen*$^{-/-}$ and *LmWT* infections showed an increase in AhR expression **(J)** upon the addition of FICZ, showing that the expression of IL-10 was FICZ-dependent. Data are represented as mean +/- SEM. Data represents one of three experiments with N=3-5 per group. *P< 0.05, ***P < 0.001, unpaired t-test

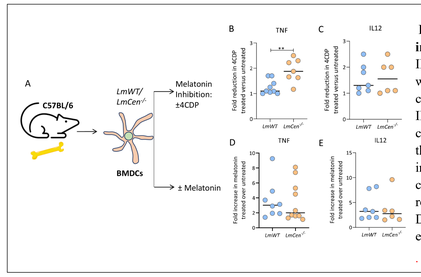

Figure 6. Validation of the role of melatonin in vaccine induced immunity. To confirm the role of melatonin in the expression of TNF and IL-12 in *LmWT* and *LmCen*$^{-/-}$ infections, BMDCs were infected overnight with *LmWT* or *LmCen*$^{-/-}$ **(A)**. After 24 hours, 4CDP was added to the culture for an additional 24 hours, and the expression levels of TNF and IL-12 were measured by RT-PCR. Treated naïve BMDCs were used for calculating fold enrichment of the analytes. Upon the addition of 4-CDP, the expression of TNF was reduced in both *LmCen-/-* and the *LmWT* infections. The reduction in TNF was significant in *LmWT* infection compared to *LmCen*$^{-/-}$ infection **(C)**. Conversely, addition of melatonin resulted an increase in TNF in both *LmCen*$^{-/-}$ and *LmWT* infections **(D)**. Data are represented as mean +/- SEM. Data represents one of three experiments with N=6-9 per group. **P < 0.01, unpaired *t*- test

CONCLUSION

- Our results show that distinct metabolic reprogramming occurs in the host cells infected with virulent or live attenuated *Leishmania* parasites.
- We have identified that the kynurenine, indole, and serotonin pathways of tryptophan metabolism are differentially regulated between the *LmWT* infection and *LmCen*$^{-/-}$ immunization.
- FICZ-AhR and kynurenine-AhR signaling are both significantly inhibited by the *LmCen*$^{-/-}$ immunization, compared to *LmWT* infection. Kynurenine-AhR and FICZ-AhR interactions are known to promote pathogenicity through increased TGF-β and IL-10 production respectively.
- In contrast, the synthesis of melatonin from tryptophan is significantly induced by the *LmCen*$^{-/-}$ immunization. Melatonin, a well-known vaccine-adjuvant, promoted a pro-inflammatory milieu though increased TNF-α in *LmCen*$^{-/-}$ immunization.

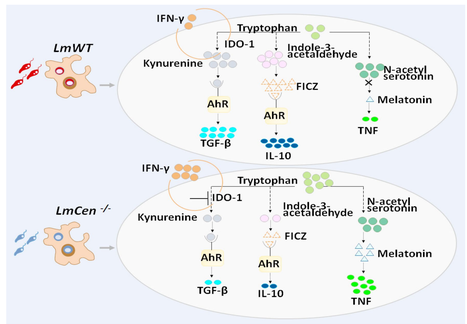

Figure 7. Graphical Summary Showcasing the three pathways of tryptophan metabolism and its immune-modulation in the *LmWT* infection (A) and the *LmCen*$^{-/-}$ (B) immunization. In the *LmWT* infection **(A)**, tryptophan metabolism is mostly used for kynurenine and indole-3-acetaldehyde synthesis, leading to the increased anti-inflammatory cytokine response through the Kynurenine-AhR and FICZ-AhR signalings. In the *LmCen*$^{-/-}$ immunization **(B)**, the kynurenine and indole-3-acetaldehyde production is inhibited, leading to the decreased activity of AhR and anti-inflammatory signals. Instead, tryptophan metabolism is mostly used for melatonin synthesis, leading to elevated levels of TNF-α and a pro-inflammatory environment that supports the vaccine immunity.

Highlights:

- ❖ Tryptophan metabolism is differentially regulated in *LmWT* and *LmCen*$^{-/-}$ infections.
- ❖ *LmCen*$^{-/-}$ infection uses tryptophan for the synthesis of TNF-α promoting melatonin.
- ❖ *LmCen*$^{-/-}$ infection downregulates kynurenine, a product of tryptophan metabolism.
- ❖ *LmWT* infection produces kynurenine that promotes anti-inflammatory activities.

REFERENCES

1. Oljuskin *et al*., Leishmania major centrin knock-out parasites reprogram tryptophan metabolism to induce a pro-inflammatory response, iScience (2023), https://doi.org/10.1016/j.isci.2023.107593.
2. Zhang *et al*. (2020). A second generation leishmanization vaccine with a markerless attenuated Leishmania major strain using CRISPR gene editing. Nat Commun 11, 3461. 10.1038/s41467-020-17154-z.
3. Nagy, C., and Haschemi, A. (2015). Time and Demand are Two Critical Dimensions of Immunometabolism: The Process of Macrophage Activation and the Pentose Phosphate Pathway. Front Immunol *6*, 164.
4. Karnovsky *et al.* (2012). Metscape 2 bioinformatics tool for the analysis and visualization of metabolomics and gene expression data. Bioinformatics *28*, 373-380.
5. Xia *et al* (2009). MetaboAnalyst: a web server for metabolomic data analysis and interpretation. Nucleic Acids Res *37*, W652-660.
6. Pang *et al* (2022). Using MetaboAnalyst 5.0 for LC-HRMS spectra processing, multi-omics integration and covariate adjustment of global metabolomics data. Nat Protoc *17*, 1735-1761.